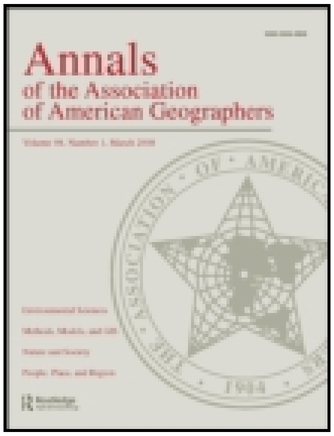

Annals of the Association of American Geographers
Publication details, including instructions for authors and subscription information:
http://www.tandfonline.com/loi/raag20

NMMI: A Mass Compactness Measure for Spatial Pattern Analysis of Areal Features

Wenwen Li[a], Tingyong Chen[b], Elizabeth A. Wentz[a] & Chao Fan[a]
[a] GeoDa Center for Geospatial Analysis and Computation, School of Geographical Sciences and Uban Planning, Arizona State University
[b] Department of Physics, Arizona State University
Published online: 10 Sep 2014.

To cite this article: Wenwen Li, Tingyong Chen, Elizabeth A. Wentz & Chao Fan (2014) NMMI: A Mass Compactness Measure for Spatial Pattern Analysis of Areal Features, Annals of the Association of American Geographers, 104:6, 1116-1133, DOI: 10.1080/00045608.2014.941732

To link to this article: http://dx.doi.org/10.1080/00045608.2014.941732

NMMI: A Mass Compactness Measure for Spatial Pattern Analysis of Areal Features

Wenwen Li,* Tingyong Chen,† Elizabeth A. Wentz,* and Chao Fan*

**GeoDa Center for Geospatial Analysis and Computation, School of Geographical Sciences and Uban Planning, Arizona State University*
†Department of Physics, Arizona State University

Spatial pattern analysis plays an important role in geography for understanding geographical phenomena, identifying causes, and predicting future trends. Traditional pattern analysis tools assess cluster or dispersed patterns of geographical features based on the distribution of nonspatial attributes. These metrics ignore the shape of spatial objects—a critical consideration. The study of shape analysis, on the other hand, measures the compactness, elongation, or convexity of an areal feature based merely on geometry, without considering patterns of its attribute distribution. This article reports our efforts in developing a new pattern analysis method called the normalized mass moment of inertia (NMMI) that integrates both shape and nonspatial attributes into the analysis of compactness patterns. The NMMI is based on a well-known concept in physics—the mass moment of inertia—and is capable of detecting the degree of concentration or diffusion of some continuous attribute on an areal feature. We termed this the mass compactness. This measure can be reduced to a shape compactness measure when the attribute is evenly distributed on the feature. We first describe the theoretical model of the NMMI and its computation and then demonstrate its good performance through a series of experiments. We further discuss potentially broad applications of this approach in the contexts of urban expansion and political districting. In the political districting context, higher NMMI of a congressional district suggests a lower degree of gerrymander and vice versa. This work makes an original and unique contribution to spatial pattern and shape analysis by introducing this new, effective, and efficient measure of mass compactness that accounts for both geometric and spatial distribution. *Key Words: compactness, mass moment of inertia, political redistricting, shape analysis, shape index, spatial distribution patterns.*

空间模式分析, 在理解地理现象、指认导因和预测未来趋势的地理中扮演重要的角色。传统模式分析工具, 根据非空间属性的分佈, 评估地理特徵的群聚或分散模式。这些度量忽略了空间物件形状这个关键的考量。另一方面, 形状分析的研究, 仅根据几何学测量一个地区的紧密度、伸张度, 或是凸起特徵, 而不考量这些属性分部的模式。本文记述我们所建立的一个名为 "常态化质量惯性矩" (NMMI) 的崭新模式分析方法之努力, 该方法同时将形态与非空间属性整合进紧密度形态的分析之中。NMMI 是根据物理学中众所週知的概念——质量惯性矩, 并可侦测一个地区特徵中部分连续属性的聚集或分散。我们将之称为质量紧密度。当属性平均分佈于特徵中之时, 此一方法可以简化为形状紧密度的测量。我们首先描述 NMMI 的理论模型及其计算, 接着透过一系列的实验, 证明其良好的表现。我们进一步在城市扩张和政治区划的脉络中, 探讨此一方法的广阔潜在应用。在政治区划的脉络中, 一个国会选区有较高的 NMMI, 意味着具有某种呈度的选区划分操纵, 反之亦然。本研究透过引进这个能够同时解释几何与空间分佈的测量质量紧密度的崭新、有效且便捷之方法, 对于空间模式和形状分析作出原创且独特的贡献。 *关键词: 紧密度、质量惯性矩, 政治再区划, 形状分析, 形状指标, 空间分佈模式。*

El análisis de patrones espaciales juega un papel muy importante en geografía para la comprensión de los fenómenos geográficos, la identificación de causas y la predicción de tendencias futuras. Con las herramientas tradicionales de análisis de patrones se evalúan los patrones de aglomeración o dispersión de rasgos geográficos basados en la distribución de atributos no espaciales. Estas métricas ignoran la forma de los objetos espaciales—una consideración crítica. El estudio del análisis de formas, por otra parte, mide el grado de compactación, alargamiento o convexidad de un rasgo espacial basado meramente en geometría, sin considerar los patrones de su distribución del atributo. Este artículo informa sobre nuestros esfuerzos para desarrollar un nuevo método de análisis de patrones denominado momento de inercia de la masa normalizado (NMMI) que integra forma y atributos no espaciales en el análisis de patrones de compacidad. El NMMI se basa en un bien conocido concepto de la física—el momento de inercia la masa—que es capaz de detectar el grado de concentración o dispersión de algún

Annals of the Association of American Geographers, 104(6) 2014, pp. 1116–1133 © 2014 by Association of American Geographers
Initial submission, September 2013; revised submission, January 2014; final acceptance, March 2014
Published by Taylor & Francis, LLC.

atributo continuo sobre un rasgo espacial. A esto nosotros lo denominamos compacidad de masa. Esta medida puede reducirse a una medida de compacidad de forma cuando el atributo se halla uniformemente distribuido sobre el rasgo. Primero describimos el modelo teórico del NMMI y su computación, para luego demostrar su buen desempeño por medio de una serie de experimentos. Adicionalmente discutimos las aplicaciones potencialmente amplias de este enfoque en los contextos de expansión urbana y regionalización política. En el contexto de la regionalización política, niveles más altos de NMMI de una circunscripción para el congreso sugieren un grado menor de *gerrymander* [es decir, un grado más bajo de manipulación de las circunscripciones electorales para favorecer un partido], y viceversa. Este trabajo hace una contribución original y única al análisis del patrón espacial y forma al introducir esta nueva, efectiva y eficiente medida de la compacidad de masa que da cuenta de la distribución geométrica y espacial. *Palabras clave: compacidad, momento de masa de inercia, regionalización política, análisis de forma, índice de forma, patrones de distribución espacial.*

Spatial analysis methods aim to quantify, model, predict, and simulate global and local characteristics of human activities and physical processes with mathematical and computational tools. GIScience researchers in tool development aim to build, evaluate, and enhance new and existing software to support spatial analysis of the associated applications (Goodchild 1992). A selection of the numerous applications that have benefited from the suite of geocomputational tools include detecting gerrymander in congressional elections (Gibbs 1961; Angel and Parent 2011), examining the variability of clusters of industrial activities (Kies, Mrosek, and Schulte 2009), modeling patterns of disease spread (Emch et al. 2012), understanding and predicting ecological processes (Tischendorf 2001), optimizing the distribution of humanitarian aid (Vitoriano et al. 2011), and simulating sustainable urban futures (Huang, Lu, and Sellers 2007).

Within these applications, identification of spatial patterns is always considered an essential component to discern regularities and anomalies of geographically referenced features. Some spatial patterns, such as cluster detection and analysis, in which the identification involves the comparison of the attribute values with nearby spatial features, are often visually intuitive on a map. Other patterns, such as those measuring the shape or arrangement of polygonal objects within a predefined geographic area, are difficult to quantify and therefore require advanced mathematical modeling or statistical analysis.

The most widely developed and applied suite of spatial pattern analysis tools, such as *k*-means cluster analysis and Getis–Ord Gi∗ (Getis and Ord 1992; Cressie 1993), are most effective for detecting clustering or dispersed patterns of point features. These tools are limited in their ability to quantify patterns for areal features such as population by census tract, habitat type, or slope by watershed boundary. Other approaches, such as Moran's *I* (Moran 1950) or Local Indicators of Spatial Autocorrelation (LISA; Anselin 1995), take areal features as input to derive a spatial weight matrix. The matrix quantifies the spatial relationship of nearby features based on contiguity or distance, ignoring the influence of the shape.

Shape—compact or not—is an essential dimension of spatial pattern (Williams and Wentz 2008). Shape here refers to a geometric representation as an outline of a geographically referenced entity such as boundaries of electoral districts, soil type boundaries, or areal delineation around disease clusters. More formally and more generally, shape is defined as an object that is independent of rotation, translation, and scale (Kendall 1984). This concept is essential for pattern analysis and comparison to determine if two or more shapes are similar to one another. Shape analysis has been used as an essential building block to model and synthesize geographic dynamics (Goodchild, Yuan, and Cova 2007), to assess the constitutionality of political districts (Rinder, Armstrong, and Openshaw 1988; Fryer and Holden 2007), to study urbanization involving large-scale changes in the land uses (Huang, Lu, and Sellers 2007; Kies, Mrosek, and Schulte 2009; Vitoriano et al. 2011), and to affect spatial cognition processes, such as wayfinding, by affecting environmental comprehension and recall (Griffith 1982; Golledge 1992; Taylor 2005; Emch et al. 2012).

Quantifying shape for analysis or comparative purposes involves a mathematical metric that assigns each unique shape with a corresponding and reproducible unique numerical representation. One such set of these metrics is the compactness measures, which quantify the density or close proximity of the defined boundary to other shapes in the data set (MacEachren 1985; Wentz 2000; Angel, Parent, and Civco 2010). A fundamental limitation of existing compactness analysis tools, such as the Isoperimetric Quotient (IPQ; Osserman 1978), is that they focus solely on the geometric boundary of a spatial object and ignore its attributes. In many real-world applications, the geographic boundaries of a region and the distribution of attributes within the region need to be incorporated into the metric. For example, in electoral redistricting, both compact shape and compact population are desired goals to avoid gerrymander (Weaver and Hess 1963). Here compact population means a concentrated population distribution, which reduces overall travel distances from each location of residence to its population center. In management science and spatial optimization, providing better coverage without increasing the size of the sales teams is always a primary goal to maintain high margins. Maximization of margins is best obtained by partitioning sales territory into compact regions in which the number of households or places a salesman needs to visit is maximized and the travel distance is minimized. In this case, both shape (compactness of sales territory) and attribute (sales activities) need to be considered in the compactness measure (Hess and Samuels 1971).

This article presents and evaluates a new approach to pattern analysis of areal features that integrates both the geometric properties and the distribution of attributes into the measurement of spatial pattern, which we call the normalized mass moment of inertia (NMMI). The mass moment of inertia (MMI) is a concept in the field of physics that assesses the dispersion of unevenly distributed attributes within an object. The mass in NMMI can be interpreted as the quantity of any descriptive attribute, such as population or salesman activity, within an areal geographic feature. The NMMI is capable of measuring the mass compactness, namely, the concentration or diffusion of a continuous attribute within the feature. It is also capable of quantifying shape compactness when the attribute is evenly distributed on the areal object. The remainder of this article includes a detailed review of existing pattern and shape measures, a mathematical model of the NMMI approach, a demonstration of the behavior of NMMI utilizing simulated data, an application of the NMMI in political redistricting using real-world data, and a conclusion that highlights our major findings and suggests future research directions.

Spatial Pattern Analysis

The literature to support our research is derived from research on geospatial pattern analysis and shape analysis. Pattern analysis research is relevant because prior studies demonstrate that both the geometric features and the associated attributes are essential to the analysis. The major shortcoming in most of the pattern analysis research, however, is that the shape of areal features is not incorporated into the geometric analysis of pattern. We therefore rely on research from shape analysis to provide the theoretical basis for this part of our study.

Pattern Analysis

According to different types of input data, spatial pattern analysis can be divided into the analysis of point features, line features, and areal features. Point pattern analysis tools discern spatial patterns through the measurement and comparison of the attribute values and geographic location rather than the geometric (e.g., shape) aspect of pattern (Boots 2003). The Getis–Ord Gi∗ statistic is a commonly used method to identify clusters of points with values higher in magnitude. *K*-means analysis detects patterns of points by examining distances between each point and its *k* closest points and compares the values with a sample of points generated from a complete spatial randomness pattern. Ripley's *k*-function (Dixon 2006) and the weighted *k*-function (Getis 1984) are also popular to determine whether a set of point features is clustered at multiple different distances.

Line Features. Line pattern analysis tools investigate the topologic and geometric variations in linear structures focusing on connectivity, flows, accessibility, and continuity (Xie and Levinson 2007). Different methods to analyze structural pattern characteristics include use of fractals to characterize line complexity (de Keersmaecker, Frankhauser, and Thomas 2003), Fourier transforms to quantify the periodic dynamics of roads (Dendrinos 1994), entropy for investigating connection patterns (Xie and Levinson 2007), and linear programming to analyze hub-and-spoke design (O'Kelly and Lao 1991). Much of the spatial line analysis research relies on graph theory methods, which eliminate line shape and focus exclusively on the type and intensity of connectivity and interactions (Derrible and Kennedy 2009).

Areal Features. A typical way to analyze patterns of areal features is to reduce the areal feature to a point and then perform analysis on these point features (Zhu and Byrt 2003). Other methods used are the join count method (which tends to be mostly for nominal features) and many of the patch-based functions as implemented in the landscape ecology software FRAGSTATS (McGarigal and Marks 1995). Some spatial autocorrelation techniques, such as Moran's *I*, LISA, and Geary's *c* (Moran 1950; Geary 1954; Anselin 1995) can also take areal feature as input. Only adjacencies of neighboring features are derived from these areal features for computing spatial covariance, however; their shapes are ignored in the analysis. One known exception is the TOSS method, which assesses whether or not features with similar attributes, orientation, shape, and size are clustered or distributed (Williams and Wentz 2008).

Shape Analysis

We categorized shape metrics into measures of shape complexity and shape compactness (Wentz 2000). Shape complexity here refers to the intricacy or amount of connectivity of the edge boundary or the fragmentation of objects. Methods used for measuring shape complexity include Fourier analysis (Moellering and Rayner 1981) and fractal analysis (B.-L. Li 2000). Shape compactness, on the other hand, measures the density or closeness of elements on an object. Compactness measures can be classified into four categories: area–perimeter measures, reference shape, dispersion of elements of area, and mass measures. We organize our review around these four categories but we provide more details on the mass measures because they form the basis of this study.

Area–Perimeter. In 1822, Ritter proposed one of the first compactness measures based on simple relationship between area and perimeter (Frolov 1975). This index does not provide normalization to a Euclidean shape; therefore, its value varies with the size of a patch, causing the known "size problem" (Farina 2006, 319–23). Modifications of the Ritter measure have been presented in many different forms (Miller 1953; Reock 1961; Schwartzberg 1965). In landscape ecology, corrected perimeter–area (CPA) is widely used to solve the size problem. CPA equals the product of a constant value (0.282) and a shape's perimeter, p, over the square root of the shape area, A. Its mathematical form is $CPA = \frac{0.282 \times p}{\sqrt[2]{A}}$. This value equals 1.0 for a perfect circle to infinity for an infinitely long and narrow shape. The iso-perimetric quotient (IPQ) approach (Osserman 1978), defined as the ratio of the area (A) of a shape to the area of a circle with the same perimeter (p) of the shape, is also a widely adopted compactness measure. Mathematically, it can be represented as $IPQ = \frac{4\pi A}{p^2}$. There are a number of variations of IPQ, such as those presented in Aslan, Gundogdu, and Arici (2007). These approaches have the advantages of being generally applicable to both vector and raster data and invariant to size change (Bação, Lobo, and Painho 2005; Patrick 2010). They suffer from sensitivity to irregular boundaries and an inability to handle holes, however (W. Li et al. 2013).

Reference Shape. The second class of measures involves the measurement of the difference between the actual shape and its reference standard shape that is deemed as most compact; for example, a circle in a vector model or a square in a raster model. One such measure is the Reock test (Reock 1961), which takes the ratio of the actual area to that of the minimum circle that completely encompasses the actual shape. Similar measures include those developed by Pounds (1972), where the perimeter instead of area was used to calculate compactness. Bottema (2000) presents a compactness index by overlaying a shape S with a circle that has the same area of S and compares the part of area in S that falls outside of the circle with S. Similar indexes include a shape index to measure parcel compactness by Amiama, Bueno, and Alvarez (2008) and Demetriou, See, and Stillwell (2013), an elongation index by Wentz (2000), and Zhao and Stough (2005). One common downside of reference shape measures is that they are inflexible to measuring shapes with frequently changing boundaries, such as a convoluted shape. Angel and Parent (2011) proposed a refined compactness measure that aims at removing the effect of geographical constraints in a shape compactness measure. The measure compares the share of area of a shape that is inside an equal-land-area circle (with area of water excluded) and is more effective in measuring compactness of political districts than the Bottema index (Angel, Parent, and Civco 2010).

Dispersion. The third set of measures was developed based on dispersion of the infinitely small elements that compose a shape to the centroid of the shape. One core concept used in developing the measure is known as the area moment of inertia (MI). Several researchers have examined the utility of the area MI test and its various forms in geographical problems. This measure overcomes the limitations of the preceding compactness measures in terms of sensitivity to size change, inflexibility to frequent shape changes, and instability to irregular shapes. Additionally, it has been demonstrated as the most effective approach to measure compactness (Weaver and Hess 1963; Massam and Goodchild 1971; Maceachren 1985).

Mass Measurements. Mass measurement, which aims at using physical models to simulate social interactions and movements, belongs to the field of social physics, which has drawn much attention and studies in the geography community (Stewart 1950; Warntz 1973; Rich and Rich 1980; Couclelis 1999; Goodchild 2004). Weaver and Hess (1963) proposed a compactness measure based on the notion of population MI. Here population is the attribute mass. It uses the continuous form of the area MI and calculates this physical quantity about the center of population gravity instead of the shape centroid. This method is capable of detecting extremely noncompact districts because the population MI is accumulated as parts of the district stay far from the population center. Although population center is used, the actual distribution of population is not considered in the computation. For this reason, it fails to provide a reasonable measure of a region that compacts population but has a noncompact shape.

In the field of management science, a number of researchers (Dantzig and Ramser 1959; Burns et al. 1985; Laporte 2009) proposed measuring compactness as the total length of the network or travel routes within each defined region. The smaller the distance is, the more compact a region is. This measure can be considered as a discrete form of the MI, because a more compact shape should not only minimize sum of distances (or squared distances) among each pair of basic elements but also minimize the sum of the MI of each basic element. For this reason, existing measures are only crude estimations of the area MI, and they only stand when the shapes and areas of basic elements are the same.

W. Li et al. (2013) proposed a robust compactness measure—the normalized moment of inertia (NMI) and demonstrated its superiority over the commonly used IPQ approach. The NMI approach involves the calculation of second MI of an area about its centroid. According to Massam and Goodchild (1971), the MI of a shape (I) about its centroid is defined as the integral of the squared distance (z_G) between an infinite small area (da) on the shape and its centroid G. Mathematically,

$$I = \int z_G^2 da. \quad (1)$$

Correspondingly, the NMI of a shape S is defined as the ratio between the MI of a circle that has the same area as S and its MI value. Suppose the shape's area is A; the NMI can be formulated as

$$NMI = \frac{I_0}{I} = \frac{A^2}{2\pi I}, \quad (2)$$

where I is the MI of S about an axis perpendicular to S and passes through its centroid G. $I_0 = A^2/2\pi$ is the MI of a reference shape—a circle with the same area of S. NMI has an interval of [0, 1], with 0 for the infinitely elongated shape and 1 for the most compact shape—a circle. This model is efficiently solved using the trapezium approach to polygon area and MI computation and has been widely applied to shape analysis in political districting (Kaiser 1966; Young 1988), the modifiable areal unit problem (MAUP; Openshaw 1977, 1978), the automatic zoning procedure (AZP; Martin, Nolan, and Tranmer 2001), and a variety of regionalization problems (Duque, Ramos, and Surinach 2007; W. Li, Church, and Goodchild 2014b).

In reality, though, essential nonspatial attributes, such as population density or wildlife distribution, are generally nonuniform. When the distribution of an attribute (we use mass to refer to the total unweighted quantity of the attribute value, such as total population) is taken into account, the NMI method for computing I in Equation 1 becomes invalid, because this measure is based purely on geometry. To address this issue, the index must be renovated to compute (1) the MI of S when mass distribution is considered and (2) the area and MI of the referenced circle. The second issue is a critical point because when some mass is not evenly distributed on S, the area of the reference shape will no longer be A. For example, if a circular shape is composed of two parts (Figure 1), the density of the red part ρ_1 is far higher than the density ρ_2 of the green part. Although the entire shape remains a circle (very compact in terms of its shape), when considering mass distribution on it, the shape of the red part would contribute much more

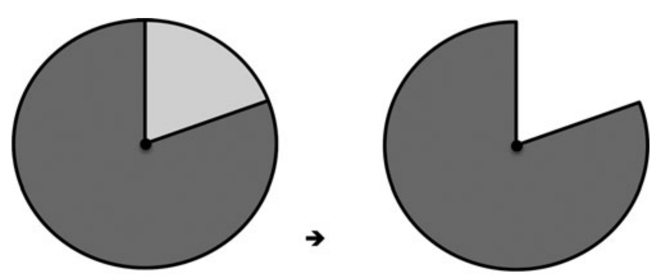

(a) A circular shape with different density distribution inside.

(b) Part of the original circular shape

Figure 1. The case of two different shapes with the same shape compactness value.

to the overall measure of compactness than the green part does. In the extreme case when $\rho_1 \gg \rho_2$, the effective area of the shape in Figure 1A becomes that shown in Figure 1B, smaller than its actual shape. Therefore, the compactness of this region will no longer be 1, referring to its circular shape. Instead, this value should be less than 1 and be the same as the NMI obtained for the shape in Figure 1B. Therefore, identifying (1) the MI of a shape when a nonuniform mass distribution is considered and (2) a reference shape on which the same amount of mass can be distributed to obtain the minimal mass MI become essential tasks for a new measure of mass compactness.

We next describe a new mathematical index based on classic physics concept of inertia mechanics to tackle the problems just identified. The MMI is introduced to compute the MI of a shape with uneven mass distribution. The MMI of a referenced shape is also derived to normalize the MMI value of a shape. The NMMI, which takes the ratio between the MMI of a shape and that of a reference shape, is introduced as a novel approach to measure the mass compactness pattern.

Mathematical Model of the NMMI Measure

Computation of NMMI involves two steps. The first step is to derive the mathematical formula for MMI of a shape and the second step is to obtain the MMI of the reference shape to obtain the normalized value. The mass is the total unweighted amount of any nonspatial attribute on a shape, such as total population or sales team activities.

This model can take both vector data and raster data as input. For vector input, a hierarchical data structure is required. Besides the boundary of the study area (i.e., congressional districts), the mass compactness of which to measure, a secondary set of areas (i.e., census tracts), or unit shapes, embedded within this study area is also required. There is an assumption that the attribute is evenly distributed on a unit shape. As for raster input data, the basic unit is a pixel and the attribute value of a pixel is the mass. The entire study area is composed of coterminous pixels that compose a shape.

MMI of a Basic Unit

The MMI is computed based on the concept of MMI:

$$I_{mass} = \int \rho(r) r^2 dv, \tag{3}$$

where I_{mass} is an object's MMI about a fixed axis, and $\rho(r)$ is the mass density at any point r. When an object is two-dimensional, we define its MMI $I_i^{G_i}$ as

$$I_i^{G_i} = \frac{A_i \int d^2 * \rho_i (r_i) * da_i}{\int \rho_i (r_i) * da_i}, \tag{4}$$

where A_i is the area of the object i, da is an infinitesimal part of area A_i, and $\rho(da_i)$ is the density function of some mass i. G_i is i's center of mass (centroid weighted by the property to measure), and d is the distance from da_i to G_i. Assuming that the attribute is evenly distributed on object i, namely, $\rho(da_i)$ is a constant ρ_i, $I_i^{G_i}$ can be simplified to

$$I_i^{G_i} = \rho_i \int d^2 da_i = \rho_i I, \tag{5}$$

where $I_i^{G_i}$ is equal to ρ times the area MI I of object i. The definition and computation of I is discussed in detail in W. Li et al. (2013). When the property is not evenly distributed on a shape, the moment of a region should be computed from its building blocks (basic units), the density of which is a constant.

MMI of a Study Area Composed of Unit Shapes

Given two coterminous unit shapes[1] u_1 and u_2, u_1 has mass m_1, area A_1, and density ρ_1, and u_2 has mass m_2, area A_2, and density ρ_2. Therefore, we have

$$\rho_1 = \frac{m_1}{A_1} \tag{6}$$

$$\rho_2 = \frac{m_2}{A_2}. \tag{7}$$

Knowing that the centroids for u_1 and u_2 are $G_1(x_1, y_1)$ and $G_2(x_2, y_2)$, respectively, as the attribute to measure is uniformly distributed on these unit shapes, G_1 and G_2 are both the area centroid and the center of mass. Given the preceding definitions, the MMI $I^{G'}$ of the new shape combining the two unit shapes becomes

$$I^{G'} = I_1^{G_1} + I_2^{G_2} + m_1 d_1^2 + m_2 d_2^2 \tag{8}$$

$$\left(x', y'\right) = \left(\frac{m_1 x_1 + m_2 x_2}{m_1 + m_2}, \frac{m_1 y_1 + m_2 y_2}{m_1 + m_2}\right) \tag{9}$$

$$\rho' = \frac{m_1 + m_2}{A'} \tag{10}$$

$$A' = A_1 + A_2, \tag{11}$$

where (x', y') is the center of mass and ρ' is the average weighted density. d_1 is the Euclidean distance between G′ and G_1, and d_2 is the Euclidean distance between G_2 and G′. When $\rho_1 = \rho_2 = \rho$, $I^{G'} = \rho I$, where I is the area MI of the region (shape that combines the two unit shapes) measuring compactness based purely on geometry.

Given this additive feature, when a shape is composed of multiple unit shapes with different density, the overall MMI can be computed through Equations 8 to 11 cumulatively.

Mass Moment of the Reference Shape

One crucial quantity in this approach is the MMI of the reference shape, which must also incorporate the nonspatial attributes as well as the geometric effect. Here, we derive the MMI I_0 of the reference shape Z_0 of a region Z. A commonly used reference shape is a circle, which has the smallest inertia and uniform distribution of an attribute. Previously, when only the shape is considered, I_0 is calculated as the MI of a circle, $I_0 = \frac{A}{2\pi}$, where A is the area of Z. The NMI, expressed as the ratio between I_0 and I, is always smaller than or equal to 1. With the mass distribution included, one would assume that I_0 is the MMI of a circle with the same area and with uniform distribution of the total mass. Unfortunately, the normalized value obtained this way exaggerates the effect of the part of the area with lower density. For instance, given a region with a square shape, when half of the region's density is much larger than the other half, the MMI of the entire shape would be the same as the part with higher density. Correspondingly, the reference shape should have an area at only half of its original shape. If we take the original area into computing I_0, the normalized value will be larger than its upper limit 1. We introduce the concept of effective area to address this issue.

When one shape is composed of two unit shapes, one has mass m_1 and the other has mass m_2, and mathematically, the effective areas of the two parts are

$$A'_1 = \frac{m_1}{m_1 + m_2}\left(A_1 + \frac{\min(\rho_1, \rho_2)}{\rho_1} A_2\right) \quad (12)$$

$$A'_2 = \frac{m_2}{m_1 + m_2}\left(A_2 + \frac{\min(\rho_1, \rho_2)}{\rho_2} A_1\right), \quad (13)$$

where function $\min(\rho_1, \rho_2)$ takes the smaller density. The effective area of each part includes its own area weighted by its mass contribution and the area contribution from the other part weighted by the density ratio. The MMI of the reference shape with the same mass and total effective area can be represented by

$$I_0 = \frac{m}{2\pi}(A'_1 + A'_2). \quad (14)$$

Substituting A'_1 and A'_2 with definitions in Equation 12 and 13, we obtain

$$I_0 = \frac{1}{2\pi}\left[\rho_1 A_1^2 + \rho_2 A_2^2 + 2\min(\rho_1, \rho_2) A_1 A_2\right]. \quad (15)$$

When $\rho_1 = \rho_2 = \rho$, I_0 can be reduced to

$$I_0 = \frac{\rho(A_1 + A_2)^2}{2\pi} = \frac{mA}{2\pi}. \quad (16)$$

Substituting I_0 in Equation 2, the NMMI result will be consistent with the NMI result, demonstrating its good performance in dealing with edge case for which $\rho_1 = \rho_2$.

For another edge case, when $\rho_1 \gg \rho_2$, the contribution of the second part to the overall compactness is negligible, meaning that the compactness of the entire shape will be the same as that of the first part of the shape. Mathematically, A'_1 becomes A_1 and A'_2 becomes 0. Therefore, $I_0 \approx \frac{m_1 A_1}{2\pi}$. According to Equation 8,

$$I^{G'} = I_1^{G_1} + I_2^{G_2} + m_1 d_1^2 + m_2 d_2^2 = I_1^{G_1} = \rho I_1^{G_1} \quad (17)$$

$$NMMI = \frac{I_0}{I^{G'}} = \frac{m_1 A_1}{2\pi \rho_1 I_1^{G_1}} = \frac{A_1^2}{2\pi I_1} = NMI. \quad (18)$$

Through the preceding analysis, we demonstrate mathematically that the proposed NMMI can handle the edge cases for which $\rho_1 = \rho_2$ and $\rho_1 \gg \rho_2$. When values of ρ_1 and ρ_2 are between these cases, I_0 in Equation 15 is the minimal MMI to reach when distributing a known mass on a two-dimensional shape. Therefore, the NMMI, a value between I_0 and I of a given object, has an interval of [0, 1], with upper bound 1 representing the most compact region and lower bound 0 representing the least compact region.

When a region is made up of multiple unit shapes ($n \geq 2$) with different uniform density, the formula for computing I_0 can be extended to

$$I_0 = \left(\sum_{i=1}^{n} \sqrt{\rho_i} A_i\right)^2 + \sum_{i<j} 2min(\rho_i, \rho_j) A_i A_j. \quad (19)$$

Given the equation for computing MMI of the referenced shape, the new index NMMI can be easily computed by applying Equation 2. Note that, with the mass distribution included, the new measure is not just a measure of shape compactness in the traditional sense; it is a measure of compactness in terms of the concentration or diffusion pattern of some mass (or some attribute value). The NMMI retains the same interval [0, 1] of the compactness measure NMI but the interpretation of the metric can be quite different. For example, for the compactness of 1, NMI simply indicates a circle, whereas in our new NMMI it can be a very irregular shape but the mass only concentrates on a circular subarea. We name this new measure the mass compactness, which covers pattern analysis broader than merely the shape compactness that the traditional compactness index covers.

Demonstration of NMMI

In this section, we use simulated data to demonstrate how the mass compactness of an areal feature changes with different distribution patterns of some attribute. The NMI approach is chosen as the benchmark index for the following reasons: (1) as discussed earlier, the NMMI, which measures the mass compactness, can reduce to the measure of shape compactness when some attribute is evenly distributed on an areal feature; therefore, there is a need for a shape compactness index to cross-compare the results; (2) the NMI approach has been demonstrated as one of the most effective approaches in measuring shape compactness through earlier studies; and (3) the MMI used in NMMI and the area MI used in NMI are both derived from Newton's law of inertia with one measuring the inertia for the whole mass and the other measuring the inertia for only the surface of an object. These two concepts are closely related to each other, and the NMMI approach, when being reduced to the measure of shape compactness, should yield the same value as the NMI.

Measuring Compactness of the Same Region with Different Mass Distribution Patterns on Simulated Data

Figure 2 illustrates several cases with different mass distribution in a square shape. In Figure 2A, the mass of a strip dominates at the center, whereas in Figure 2B the mass concentrates on a subsquare at the center. In Figure 2C, the mass has some distribution cut by a corner of a square and the mass dominates along the diagonal line in Figure 2D. If the NMI model is used to calculate the compactness, these four cases should give the same compactness of a square, 0.955, but obviously we missed the most important information of mass distribution.

Based on our new NMMI model, the compactness of these shapes depends on the density, χ, of the purple area. The calculated compactness is shown in Figure 3 where the density of the white area $\rho_{white} = 1$. For $\ln(\chi) = 0$, where $\chi = 1$, this large square region has uniform mass distribution. Therefore, all cases have the same compactness of 0.955, as expected, demonstrating that our NMMI model can be correctly reduced to the previous NMI model. As χ increases, the compactness of the case in Figure 3A decreases monotonically and eventually reaches a constant value of 0.367, the NMI compactness of the purple area inside. For the case in Figure 3B, one notes that the compactness is a constant for all the values of χ. This is expected because the purple area has the same shape as the outside square. The compactness of the case Figure 3D also decreases monotonically as χ increases but in a different manner from that of the case in Figure 3A because of a different shape of the purple area in Figure 3D. The purple area in Figure 3D is wider than that in Figure 3A, which leaves a large compactness of 0.496 at large χ. Interestingly, the compactness of the case in Figure 3C increases as χ increases, because the purple shape is more compact than a square. In fact, the NMI compactness of the purple shape is 0.986, which is exactly the limit value we get at large χ in Figure 3.

An important feature in Figure 3 is the χ value. The compactness of all the areas changes mostly on the interval of $\chi = [1, 400]$, indicating the effect of the mass distribution is important in this region. Indeed, for $\chi = 2$, the compactness of the cases in Figure 3A and Figure 3D is 0.73 and 0.62, respectively, very different from the value of 0.955 without the mass distribution included. This demonstrates that it is important to take the mass distribution effect into account when calculating compactness.

Measuring Compactness of a Region with More Complex Patterns

In an urban expansion scenario, a small star town appears in the vacinity of a major city and expands over time. The compactness of the process can be very important for measuring the region's transportation efficiency or use as a reference for setting up fire stations, retail stores, hospitals, and other public facilities to better serve its residents. Of course, an important factor,

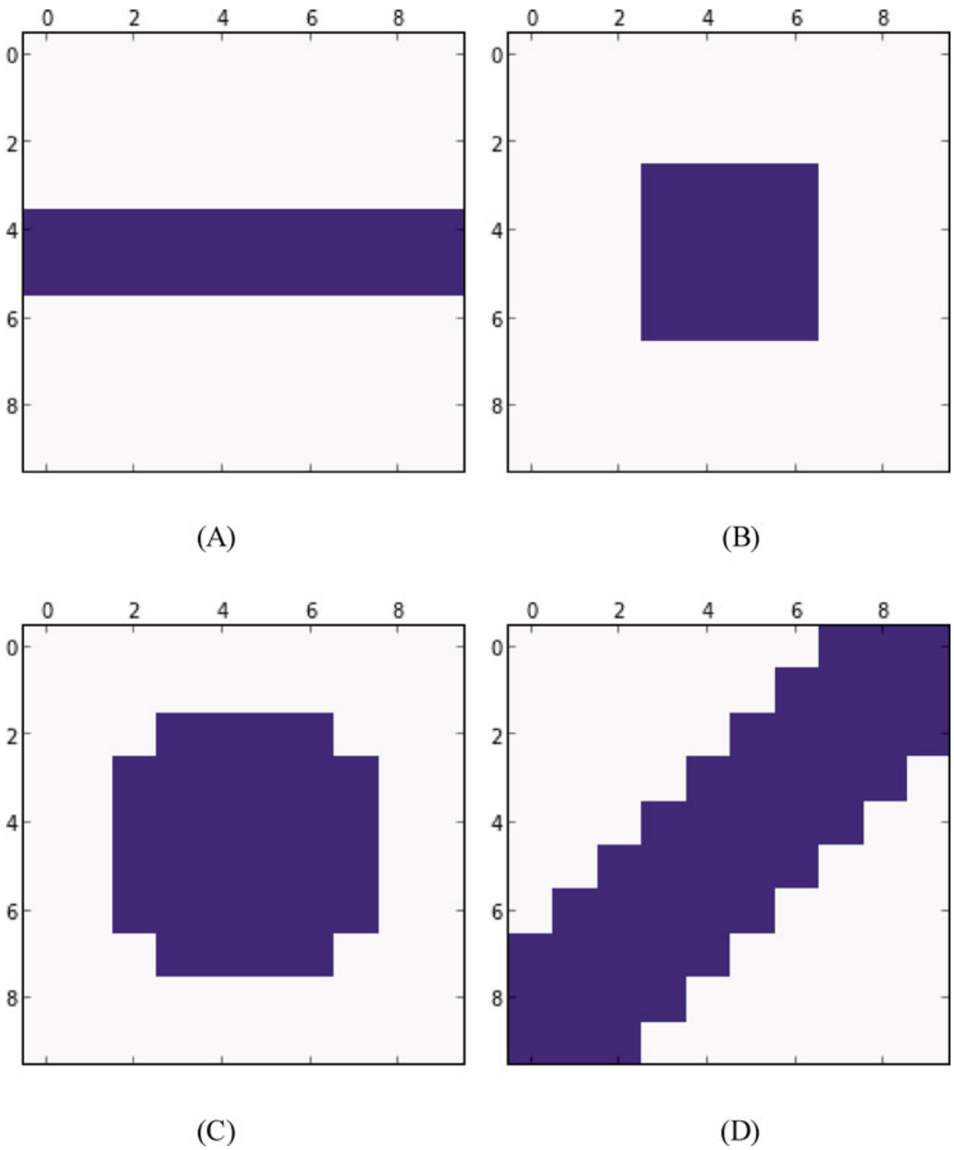

Figure 2. One shape with different density distribution patterns. (Color figure available online.)

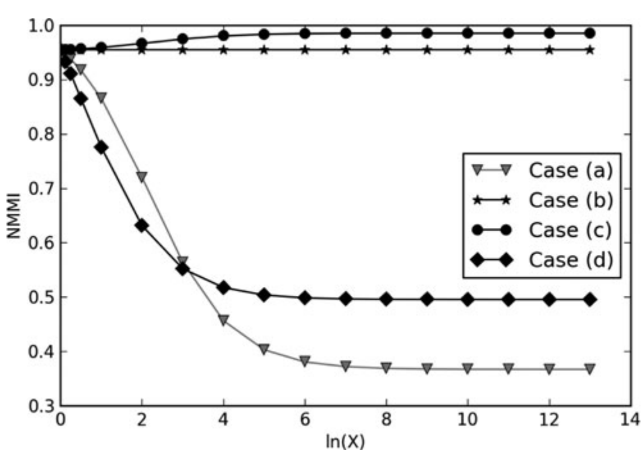

Figure 3. The normalized mass moment of inertia (NMMI) compactness of the cases illustrated in Figure 2 as a function of the density X.

the population density, must be taken into account for calculating the region's compactness. We simulated the scenarios in Figure 4. In a 15 × 30 rectangular region, there are two near-circular shapes. Initially (at time t_0), only one city A was in the west side of the rectangular region. At time t_1, a new city B was developed at the northeast corner of the region and started to attract immigrants. Next, the population of city B gradually grows through time ($t_2, \ldots, t_{n-1}$). At t_n, city B's population becomes the same as that of city A. From t_n, city B's population surpasses city A. The population density of the white area in the rectangular is set to be a low constant value 1, indicating its very sparse population distribution. Whereas the population density of city A is a consistently high value ($\ln(\rho_A) = 20$), the population density of city B is a variant X, which starts at

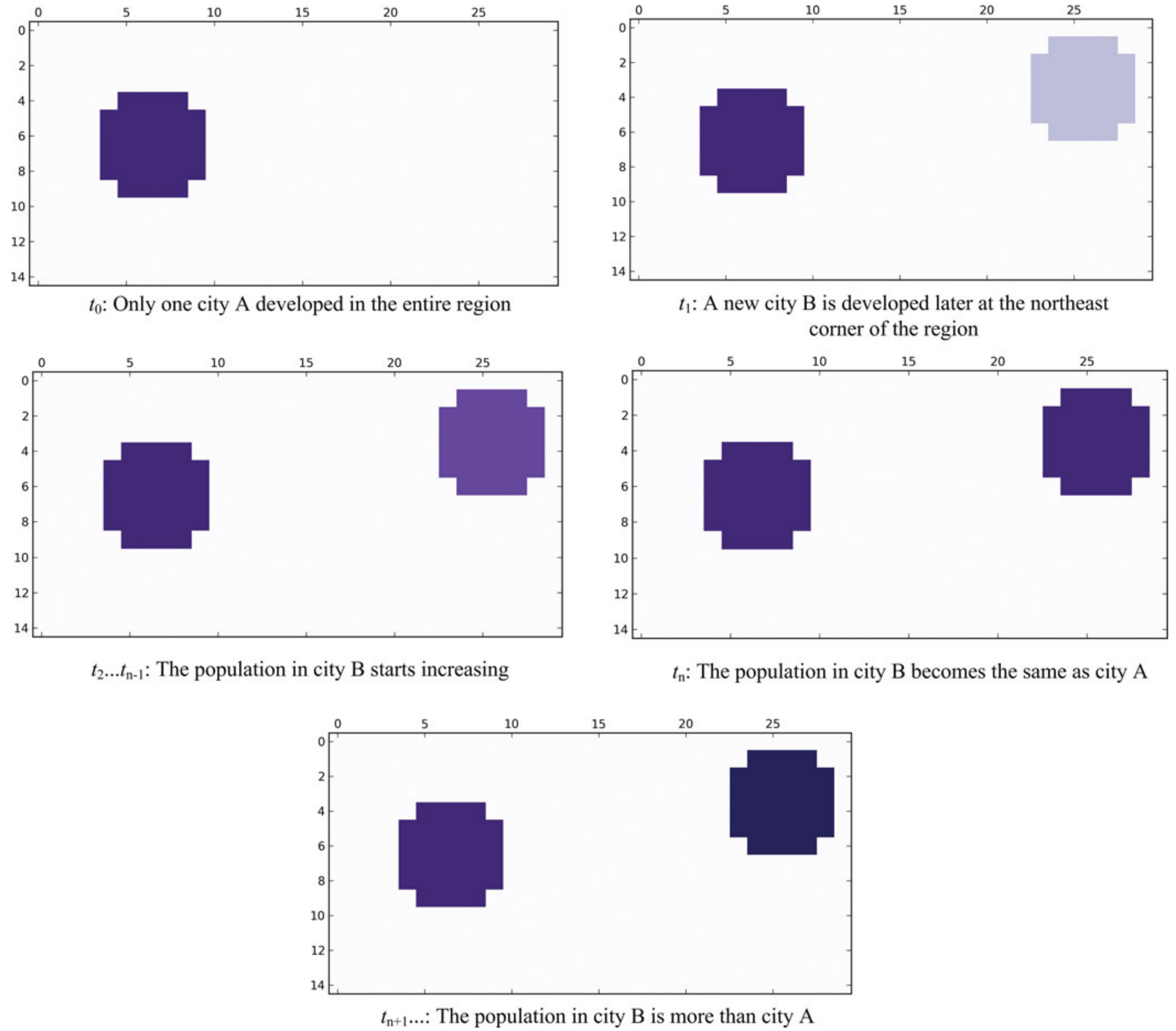

Figure 4. Urban development scenario. (Color figure available online.)

1 and keeps increasing until it reaches ($\ln(X) = 30$). Let us study the compactness of this area through the development of city B.

The calculated results are shown in Figure 5. The blue curve shows the expected NMI compactness 0.764, when the population density distribution is not included. When the NMMI approach is applied, the compactness value demonstrates an interesting variation. When the population of city B is much less than that of city A ($< \ln(X) = 6$, the first seven points on the red curve), the effect brought by city B is negligible. As the population density of B increases, its effect on the overall compactness starts to appear, indicated by the gradual decline of values in the curve. When city B's population reaches as high as city A, the minimal compactness value (0.10) is achieved. In this case, no shapes will take a leading effect in the overall compactness measure and the population is the most dispersed. When city B's population goes beyond that of city A after t_n, the shape of city B, which is a near circle, starts to take more effect and the compactness value of the whole region increases again. Another interesting finding is the symmetric change of the curve around t_n, when city A and city B's population and density become the same. This phenomenon shows that the proposed algorithm is not sensitive to the absolute positioning of dense areas; only the pattern matters.

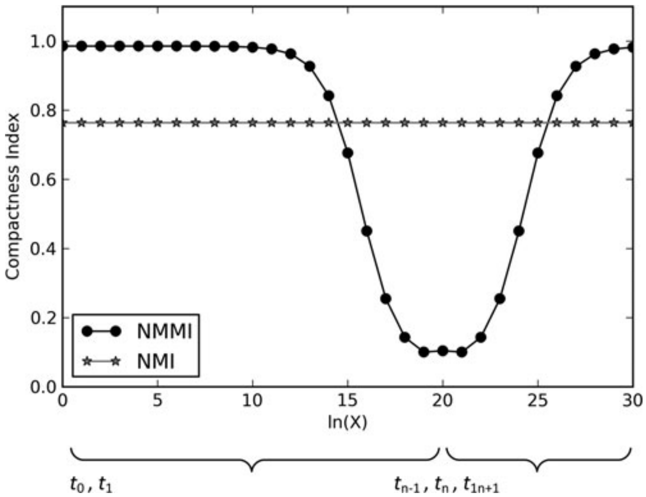

Figure 5. Variation as density distribution of the region changes.

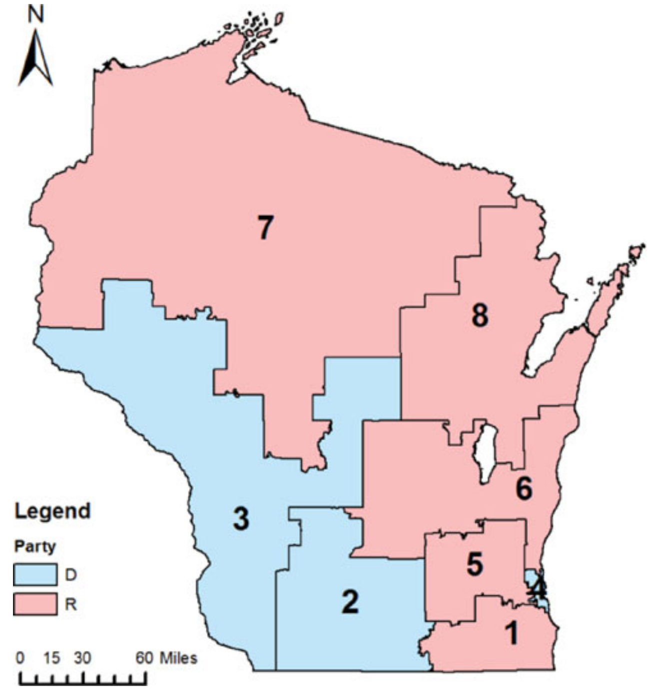

Figure 6. Wisconsin's congressional districts: Districts in blue are Democrat seats and districts in red are Republican seats. (Color figure available online.)

An Application of NMMI in Political Districting

This section introduces an empirical study that (1) compares the use of NMI and NMMI in assessing compactness of Wisconsin's congressional districts and (2) shows the effectiveness of NMMI in the process of political redistricting to prevent gerrymander. Population distribution is an important factor to be considered in this case because not only the shape of the congressional districts needs to be compacted but also the population (Hess and Samuels 1971). This is because if the population is largely diffused in an elongated subregion even on a compact shape, large bypassed communities will be generated, making voters stay far away from the population center, the presumed location of a district's electoral seat. This could also indicate the intentional partitioning of people belonging to the same political party to win the election—a typical case of gerrymandering.

Because the compactness of a shape is visible on a map but the mass compactness is not, the NMI is applied as a benchmark index to demonstrate the differences in compactness measures when population distribution is considered.

Assessing Compactness of Congressional Districts of Wisconsin

Compactness is always is an important criterion to evaluate gerrymander in congressional districts. The 113th congressional district in Wisconsin was selected as the study area because of its egregious gerrymandering. In this study, we demonstrate how to use the proposed NMMI measure to suggest the possible existence of gerrymandering. The NMIs for all congressional districts are also computed as reference data indicating the compactness of regions' shape.

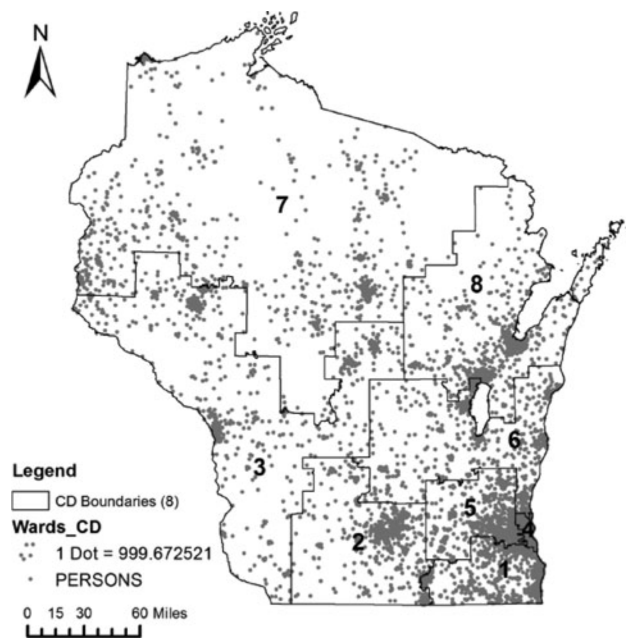

Figure 7. Dot density map for congressional districts in Wisconsin. Each dot represents 1,000 people in a ward.

We obtained the 113th congressional district data from the state legislative districting website (http://legis.wisconsin.gov/ltsb/redistricting/redistricting.htm). Figure 6 shows the overview of the eight congressional districts (CDs) in Wisconsin. Among these CDs, five of them (CD1, CD5, CD6, CD7, and CD8) are held by Republicans (in red) and the remaining three are held by Democrats (in blue). Each district has approximately 710,803 people (based on the 2010 U.S. Census). Data for wards, which are basic units for drawing CDs, were retrieved from the same website. Figure 7 depicts a dot density map of the entire state and Figure 8 shows the population distribution in each district based on wards. Visually, it can be seen

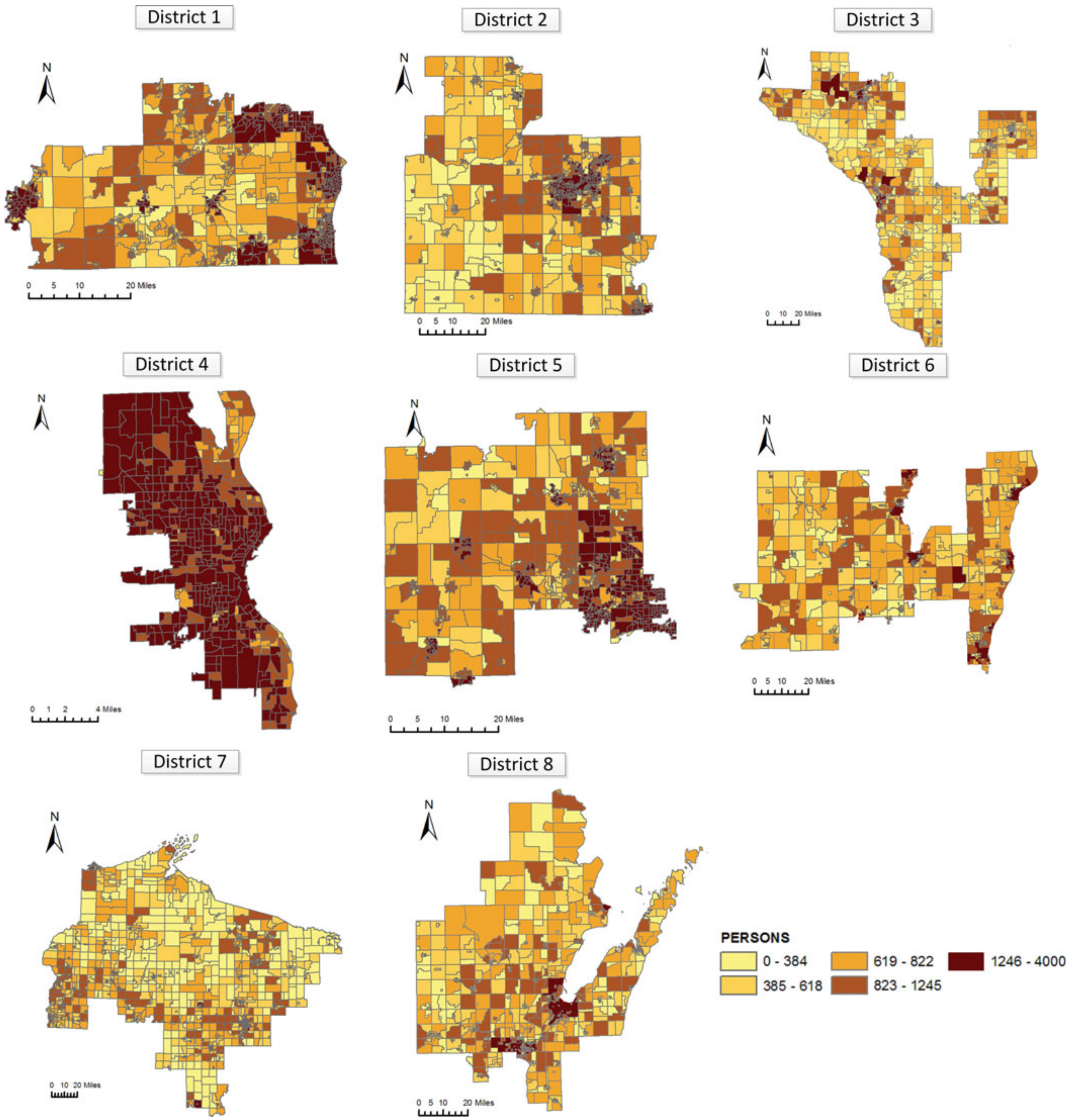

Figure 8. Shape and population distribution of each congressional district. All districts use the same color scheme, as shown at the bottom of all figures. (Color figure available online.)

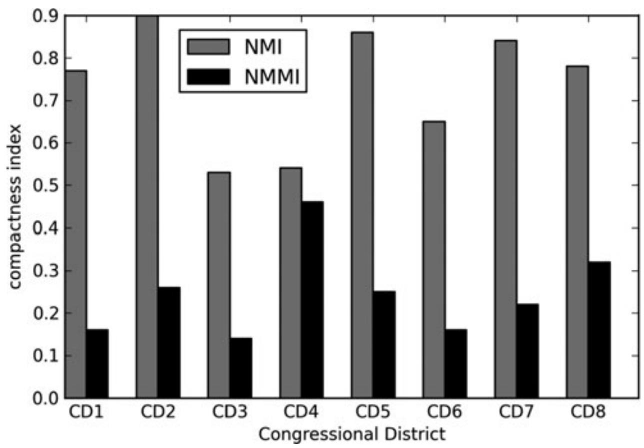

Figure 9. Comparison of compactness of eight congressional districts in Wisconsin using normalized moment of inertia (NMI) and normalized mass moment of inertia (NMMI).

that although CD4's shape is not very compact, the population is highly concentrated within the district. Therefore, it should receive a high NMMI score. In contrast, CD3, which has a Y shape and a quite diffused distribution of population, should receive a low NMMI score.

To verify our observation, both the NMMI and NMI on the shape files of the districts were applied and the results are displayed in Figure 9. When only the geometric shape of these CDs is considered (using NMI), District 2 receives the highest value in compactness—0.9—followed by Districts 5, 7, 8, 1, and 6. District 3, which has a Y shape, and District 4, which has an elongated shape and an irregular boundary, receive the lowest values (0.53 for District 3 and 0.54 for District 4) on the NMI measure. Although District 7 is associated with islands, as these islands are relatively small compared to the mainland, and the overall shape of District 7 is close to a circle, it is still considered to be compact.

When the NMMI measure is applied, the compactness value distribution changes. First, the overall trend in Figure 9 and Table 1 shows that the compactness values, when considering population distribution on a CD, all decrease from the original NMI measure. This is not surprising, because in reality it is difficult to have uniform population distribution within a large region. This nature of uneven distribution causes the lower value in the compactness measure. Recall from earlier experiments that when the property to measure shows a uniform distribution on a shape, the NMI and NMMI yield the same value. Second, District 4, which has almost the least compact shape over all CDs, is now ranked as the most compact region when population distribution is considered. Several reasons explain this turnover in compactness measure. First, District 4 is 100 percent urban area, which is much denser than other CDs. The area of District 4 is only 129 square miles, or 0.0018 percent of the entire state. Although a smaller area does not mean that the area could be more compact, it does show from Figure 9 that this CD's population is much more concentrated than the others. Second, looking at the pattern of population distribution, most of the population is located in middle to upper north Milwaukee in this district. The city of Glendale, which is located in the northeast of the district, has much less population. Due to this fact, the population exchange between the northeast areas and the main district area is minimal, indicating stronger voter proximity and a lower degree of gerrymandering in this district.

The worse cases occur for Districts 1, 3, and 6. All have more a compact shape than District 4, according to NMI. When considering population distribution, however, their NMMI compactness scores become much lower than that of District 4, indicating a higher degree of gerrymandering. This is because population is widely dispersed in these districts or areas of dense population even appear along the boundaries of some districts,

Table 1. Compactness value distribution of Wisconsin congressional districts (CDs) using normalized moment of inertia (NMI) and normalized mass moment of inertia (NMMI) approaches

	CD1	CD2	CD3	CD4	CD5	CD6	CD7	CD8
NMMI	0.16	0.26	0.14	0.46	0.25	0.16	0.22	0.32
NMI	0.77	0.90	0.53	0.54	0.86	0.65	0.84	0.78

M	NMI	NMMI
Republican CDs	0.48	0.22
Democratic CDs	0.72	0.29

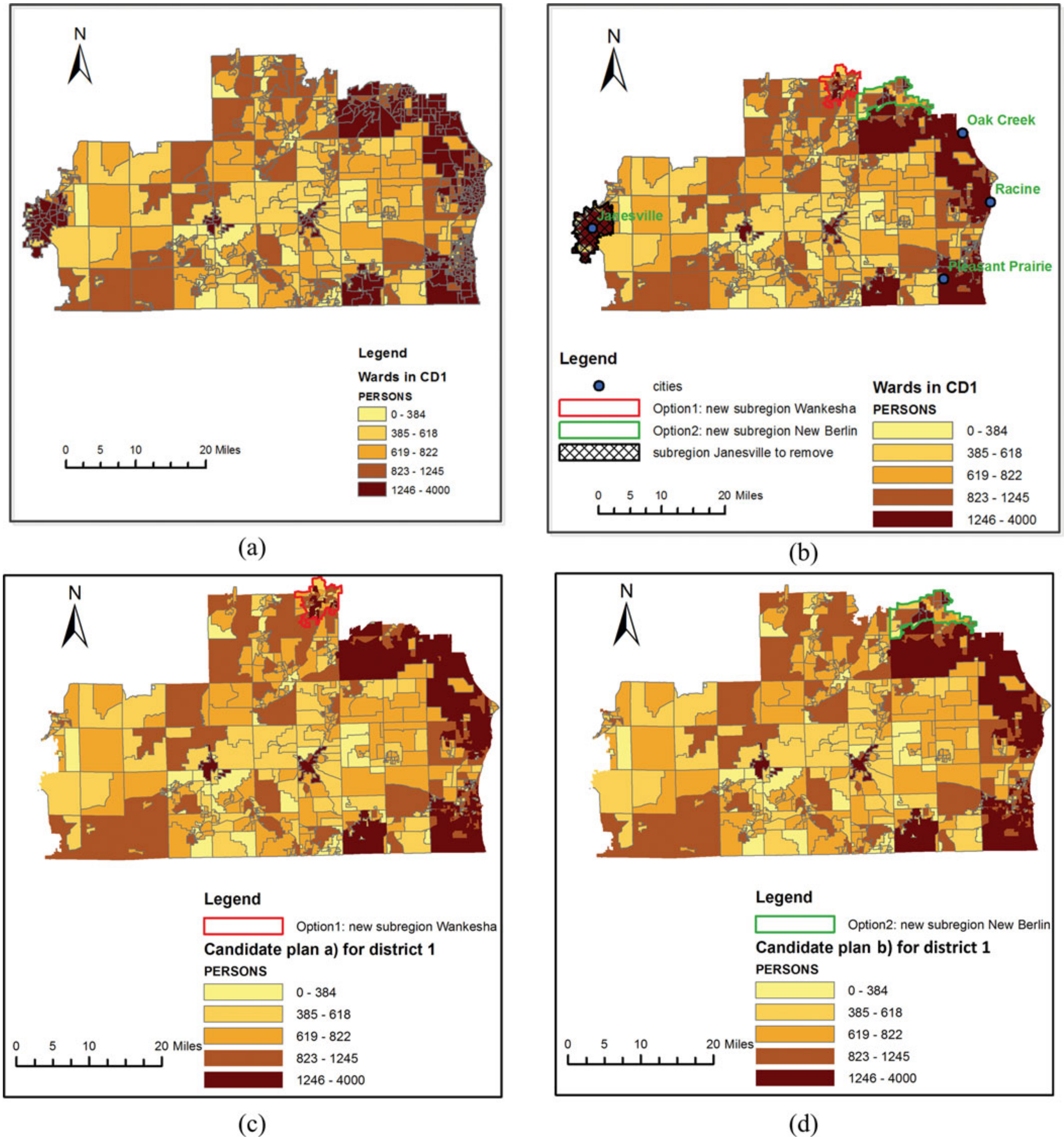

Figure 10. Possible adjustments for Congressional District 1 according to population distribution: (A) Current CD1; (B) two plans to redraw boundaries of CD1 in a redistricting process; (C) CD1 after implementing Waukesha plan; (D) CD1 after implementing the New Berlin plan. (Color figure available online.)

such as District 1, making them less compact than those measured purely on shape. Among these three districts, District 3 receives consistently low values from both the NMI and the NMMI measures, coming from its least compact shape and the dispersed population distribution on the shape. For Districts 2, 5, and 8, despite their spread-out distribution of population, there are always clear clusters of high-density areas near their population centers: Madison in District 2, the northern Milwaukee suburb in the southeast corner of District 5, and Green Bay in District 8. These clusters contribute positively to the measure of mass and population compactness because trips to the population center are minimized for these clusters.

Table 1 also shows the mean values of compactness using both the NMI and the NMMI measure. The mean NMMI of Democratic districts is 0.29, 32 percent higher than the mean NMMI of the Republican districts, suggesting a lower degree of gerrymandering among the Democratic districts and a higher degree of gerrymandering in Republican districts. This finding coincides with that found in Fischer (2013). The NMI measure, however, yields the opposite conclusion. From the preceding analysis, one can tell that the NMMI measure can well be applied to detect the possible existence of gerrymandering: The higher value the NMMI is, the less gerrymandered a CD is and vice versa.

Implication of NMMI Results in Political Redistricting

The preceding example demonstrates the feasibility of using the proposed NMMI to measure compactness of a CD. Besides this capability, the NMMI measure can also be applied for designing a better districting plan, which aims at achieving better compactness in contiguous and equally populous regions. Taking CD1 as an example, there are two major local population centers located along its boundary: Janesville near the west boundary and the one including Oak Creek, Racine, and Pleasant Prairie along the east boundary. Due to this east–west dispersed distribution pattern, the compactness value is very low for District 1 even though it has a compact shape (NMI yields to 0.9).

Adjusting the geographical boundaries according to its population distribution and the NMMI measure, a better plan might be generated. Figure 8 shows optional region partition plans by removing the Janesville area (crosshatch region in black) of 63,532 people from District 1 and adding either of the two candidate subregions—Waukesha (with a red boundary in Figure 8) and New Berlin (with a green boundary in Figure 8)—in attempting to satisfy the equal population requirement. The two candidate plans, which we called the Waukesha plan and the New Berlin plan, are demonstrated in Figure 9. Both subregions are "borrowed" from District 5, the neighbor of District 1 to the north. The purpose of generating new plans is to improve the mass compactness of this district by making the highly dense area within the district closer instead of diffused.

Both the NMI and NMMI are applied on the candidate districts, and the results were compared with the original plan. For the pure shape compactness measure, the NMI, the Waukesha plan yields a compactness value of 0.71 and the New Berlin plan yields a compactness value of 0.75, both slightly smaller than that of the original plan (0.77). In terms of merely the shape, both plans would not be favorable because they make District 1 less compact. It does compact the district's population, however. The NMMI for the Waukesha plan is 0.21 and the NMMI for the New Berlin plan is 0.22, and these plans introduce a 30 percent and 35 percent increase to the NMMI of the original plan, respectively. Although both candidates' plans tend to include more concentrated population on the east side of the district, the higher value that the New Berlin plan obtains compared to the Waukesha plan makes sense because the New Berlin plan makes the cluster pattern more obvious than the Waukesha plan, which adds a population center a bit further to the existing population center in the east.

Through the preceding analysis, we found that both candidate plans obtained using the NMMI measure are potentially better plans than the original partition. Undoubtedly, borrowing subregions from District 5 will lead to a population decrease for that region and repartitioning of one CD always involves the repartitioning of all adjacent districts. The repartitioning process is actually a redistricting and regionalization problem (W. Li, Church, and Goodchild 2014a). Our aim is to demonstrate that integrating the NMMI compactness measure into the redistricting process has the potential of yielding results that satisfy the equal population objective and at the same time are more compact to avoid gerrymandering.

Conclusion and Future Work

This article reports our contribution to developing a new areal unit pattern measure, the NMMI, based on MMI for discerning the concentration or the diffusion pattern of a continuous attribute on an areal feature. The motivation for this work comes from the effective yet limited function provided by the NMI (W. Li et al. 2013), which assumes the even distribution of a property on a shape. Using the proposed measure for assessing compactness has the following advantages.

This measure integrates both geometry and nonspatial attributes into the assessment of spatial compactness patterns, thereby enhancing traditional nonspatial statistical analysis tools by incorporating geometry information and existing shape analysis tools by integrating distribution pattern of some attribute. As the NMMI in essence measures the dispersion of basic elements distributed on an areal shape, it becomes especially useful for applications in which compact activities or compact interactions are desired.

Although different in mathematical formulation, the computation of the NMMI inherits and carries the strength of the computation of the NMI. First, the NMMI is computationally efficient. Its efficiency lies in the additive nature of Newton's law of inertia (Earman and Friedman 1973), from which both measures are derived. When the shape of a spatial object changes (i.e., including a new subarea or removing an existing subarea), there is no need to recompute the compactness of all the subareas that make up the shape. Only the MI of subarea, the original shape, and the change of MI brought by merging or removing the subarea need to be computed. Furthermore, the NMMI is robust toward positioning errors of the vertices on the boundary of a spatial object, preventing errors from data uncertainty, which is unavoidable in practice. The NMMI is also able to take both vector and raster data as input for analyzing the compactness pattern. This capability allows the widespread adoption of the NMMI approach, such as census-related analysis in which vector data are more often used or ecological applications in which raster data are the major data source. Finally, the NMMI is able to handle a shape that has holes or islands, such as the basswood island in Wisconsin CD7.

Future efforts will involve distributing open source code to the geography community. We will further improve the algorithm to integrate real transportation networks into the analysis, such that the straight-line distance between each element pair used in the computation can be replaced by the network distance, either the shortest path or the quickest path according to different application needs. We will also investigate the applicability of the proposed mass compactness measure in a special area of spatial pattern analysis, landscape pattern analysis, in which most pattern measures still use statistical tools that ignore the shape of spatial features or only basic shape factors, such as the area perimeter ratio in the FRAGSTATS tool (McGarigal and Marks 1995).

Funding

This article was in part supported by an Arizona State University College of Liberal Arts and Sciences Faculty Seed grant.

Note

1. A unit shape is represented as a polygon and unit shapes could be different, and the mass is evenly distributed on a unit shape.

References

Amiama, C., J. Bueno, and C. Alvarez. 2008. Influence of the physical parameters of fields and of crop yield on the effective field capacity of a self-propelled forage harvester. *Biosystems Engineering* 100 (2): 198–205.

Angel, S., and J. Parent. 2011. Non-compactness as voter exchange: Towards a constitutional cure for gerrymandering. *Northwestern Interdisciplinary Law Review* 4:89–145.

Angel, S., J. Parent, and D. L. Civco. 2010. Ten compactness properties of circles: Measuring shape in geography. *Canadian Geographer-Geographe Canadien* 54 (4): 441–61.

Anselin, L. 1995. Local indicators of spatial association—LISA. *Geographical Analysis* 27 (2): 93–115.

Aslan, S. T., K. S. Gundogdu, and I. Arici. 2007. Some metric indices for the assessment of land consolidation projects. *Pakistan Journal of Biological Sciences* 10 (9): 1390–97.

Bação, F., V. Lobo, and M. Painho. 2005. Applying genetic algorithms to zone design. *Soft Computing* 9 (5): 341–48.

Boots, B. 2003. Developing local measures of spatial association for categorical data. *Journal of Geographical Systems* 5 (2): 139–60.

Bottema, M. J. 2000. Circularity of objects in images. In *International Conference on Acoustic, Speech and Signal Processing*, vol. 4, 2247–50. Istanbul: IEEE.

Burns, L. D., R. W. Hall, D. E. Blumenfeld, and C. F. Daganzo. 1985. Distribution strategies that minimize transportation and inventory costs. *Operations Research* 33:469–90.

Couclelis, H. 1999. Space, time, geography. *Geographical Information Systems* 1:29–38.

Cressie, N. 1993. Statistics for spatial data. *Terra Nova* 4 (5): 613–17.

Dantzig, G. B., and J. H. Ramser. 1959. The truck dispatching problem. *Management Science* 6 (1): 80–91.

De Keersmaecker, M. L., P. Frankhauser, and I. Thomas. 2003. Using fractal dimensions for characterizing intra-urban diversity: The example of Brussels. *Geographical Analysis* 35 (4): 310–28.

Demetriou, D., L. See, and J. Stillwell. 2013. A parcel shape index for use in land consolidation planning. *Transactions in GIS* 17 (6): 861–82.

Dendrinos, D. S. 1994. Traffic-flow dynamics: A search for chaos. *Chaos, Solitons & Fractals* 4 (4): 605–17.

Derrible, S., and C. Kennedy. 2009. Network analysis of world subway systems using updated graph theory. *Transportation Research Record: Journal of the Transportation Research Board* 3 (1): 17–25.

Dixon, P. M. 2006. Ripley's K function. *Encyclopedia of Environmetrics* 3: 1796–1803.

Duque, J. C., R. Ramos, and J. Surinach. 2007. Supervised regionalization methods: A survey. *International Regional Science Review* 30 (3): 195–220.

Earman, J., and M. Friedman. 1973. The meaning and status of Newton's law of inertia and the nature of gravitational forces. *Philosophy of Science* 40:329–59.

Emch, M., E. D. Root, S. Giebultowicz, M. Ali, C. Perez-Heydrich, and M. Yunus. 2012. Integration of spatial and social network analysis in disease transmission studies. *Annals of the Association of American Geographers* 102 (5): 1004–15.

Farina, A. 2006. *Principles and methods in landscape ecology: Towards a science of the landscape*. Dordrecht, The Netherlands: Springer.

Fischer, B. 2013. Wisconsin's "shameful" gerrymander of 2012. *PRWatch*. http://www.prwatch.org/news/2013/02/11968/wisconsins-shameful-gerrymander-2012 (last accessed 8 January 2014).

Frolov, Y. S. 1975. Measuring the shape of geographical phenomena: A history of the issue. *Soviet Geography* 16 (10): 676–87.

Fryer, R. G., Jr., and R. T. Holden. 2007. *Measuring the compactness of political districting plans*. http://www.nber.org/papers/w13456 (last accessed 1 September 2013).

Geary, R. C. 1954. The contiguity ratio and statistical mapping. *The Incorporated Statistician* 5 (3): 115–46.

Getis, A. 1984. Interaction modeling using second-order analysis. *Environment and Planning A* 16 (2): 173–83.

Getis, A., and J. K. Ord. 1992. The analysis of spatial association by use of distance statistics. *Geographical Analysis* 24 (3): 189–206.

Gibbs, J. P. 1961. A method for comparing the spatial shapes of urban units. In *Urban research methods*, ed. J. P. Gibbs, 99–106. Princeton, NJ: Van Nostrand.

Golledge, R. G. 1992. Place recognition and wayfinding: Making sense of space. *Geoforum* 23 (2): 199–214.

Goodchild, M. F. 1992. Geographical information science. *International Journal of Geographical Information Systems* 6 (1): 31–45.

———. 2004. GIScience, geography, form, and process. *Annals of the Association of American Geographers* 94 (4): 709–14.

Goodchild, M. F., M. Yuan, and T. J. Cova. 2007. Towards a general theory of geographic representation in GIS. *International Journal of Geographical Information Science* 21 (3): 239–60.

Griffith, D. A. 1982. Geometry and spatial interaction. *Annals of the Association of American Geographers* 72 (3): 332–46.

Hess, S. W., and S. A. Samuels. 1971. Experiences with a sales districting model: Criteria and implementation. *Management Science* 18:P41–P54.

Huang, J., X. Lu, and J. M. Sellers. 2007. A global comparative analysis of urban form: Applying spatial metrics and remote sensing. *Landscape and Urban Planning* 82 (4): 184–97.

Kaiser, H. F. 1966. An objective method for establishing legislative districts. *Midwest Journal of Political Science* 10 (2): 200–13.

Kendall, D. G. 1984. Shape manifolds, procrustean metrics, and complex projective spaces. *Bulletin of the London Mathematical Society* 16 (2): 81–121.

Kies, U., T. Mrosek, and A. Schulte. 2009. Spatial analysis of regional industrial clusters in the German forest sector. *International Forestry Review* 11 (1): 38–51.

Laporte, G. 2009. Fifty years of vehicle routing. *Transportation Science* 43 (4): 408–16.

Li, B.-L. 2000. Fractal geometry applications in description and analysis of patch patterns and patch dynamics. *Ecological Modelling* 132 (1): 33–50.

Li, W., R. L. Church, and M. F. Goodchild. 2014a. An extendable heuristic framework to solve the p-compact-regions problem for urban economic modeling. *Computers, Environment and Urban Systems* 43:1–13.

———. 2014b. The p-compact-regions problem. *Geographical Analysis* 46 (3): 250–73.

Li, W., M. F. Goodchild, and R. Church. 2013. An efficient measure of compactness for two-dimensional shapes and its application in regionalization problems. *International Journal of Geographical Information Science* 27 (6): 1227–50.

Li, X., W. Zhou, and Z. Ouyang. 2013. Forty years of urban expansion in Beijing: What is the relative importance of physical, socioeconomic, and neighborhood factors? *Applied Geography* 38:1–10.

Maceachren, A. M. 1985. Compactness of geographic shape—Comparison and evaluation of measures. *Geografiska Annaler Series B: Human Geography* 67 (1): 53–67.

Martin, D., A. Nolan, and M. Tranmer. 2001. The application of zone-design methodology in the 2001 UK Census. *Environment and Planning A* 33 (11): 1949–62.

Massam, B. H., and M. F. Goodchild. 1971. Temporal trends in the spatial organization of a service agency. *Canadian Geographer* 15:193–206.

McGarigal, K., and B. J. Marks. 1995. Spatial pattern analysis program for quantifying landscape structure. General Technical Report PNW-GTR-351, U.S. Department of Agriculture, Forest Service, Pacific Northwest Research Station.

Miller, V. C. 1953. *A quantitative geomorphic study of drainage basin characteristics in the Clinch Mountain area*. New York: Department of Geology, Columbia University.

Moellering, H., and J. N. Rayner. 1981. The harmonic analysis of spatial shapes using dual axis Fourier shape analysis (DAFSA). *Geographical Analysis* 13 (1): 64–77.

Moran, P. A. 1950. Notes on continuous stochastic phenomena. *Biometrika* 37 (1–2): 17–23.

O'Kelly, M. E., and Y. Lao. 1991. Mode choice in a hub-and-spoke network: A zero-one linear programming approach. *Geographical Analysis* 23 (4): 283–97.

Openshaw, S. 1977. Geographical solution to scale and aggregation problems in region-building, partitioning and spatial modeling. *Transactions of the Institute of British Geographers* 2 (4): 459–72.

———. 1978. Empirical-study of some zone-design criteria. *Environment and Planning A* 10 (7): 781–94.

Osserman, R. 1978. Isoperimetric inequality. *Bulletin of the American Mathematical Society* 84 (6): 1182–1238.

Patrick, K. T. 2010. *A mathematical model for political districting with compactness consideration and an application to Kentucky Senate districting*. Urbana–Champaign: University of Illinois.

Pounds, N. 1972. *Political geography*. New York: McGraw-Hill.

Reock, E. C. 1961. A note: Measuring compactness as a requirement of legislative apportionment. *Midwest Journal of Political Science* 5 (1): 70–74.

Rich, D. C., and D. Rich. 1980. *Potential models in human geography*. Norwich, UK: University of East Anglia.

Rinder, D., A. Armstrong, and S. Openshaw. 1988. The domesday machine: A nationwide geographical information system. *Geographical Journal* 154 (1): 56–68.

Schwartzberg, J. E. 1965. Reapportionment, gerrymanders, and the notion of compactness. *Minnesota Law Review* 50:443.

Stewart, J. Q. 1950. The development of social physics. *American Journal of Physics* 18:239.

Taylor, H. A. 2005. Mapping the understanding of understanding maps. In *The Cambridge handbook of visuospatial thinking*, ed. P. Shah and A. Miyake, 295–333. New York: Cambridge University Press.

Tischendorf, L. 2001. Can landscape indices predict ecological processes consistently? *Landscape Ecology* 16 (3): 235–54.

Vitoriano, B., M. T. Ortuño, G. Tirado, and J. Montero. 2011. A multi-criteria optimization model for humanitarian aid distribution. *Journal of Global Optimization* 51 (2): 189–208.

Warntz, W. 1973. New geography as general spatial systems theory: Old social physics writ large. *Directions in Geography* 488:89.

Weaver, J. B., and S. W. Hess. 1963. A procedure for nonpartisan districting: Development of computer techniques. *The Yale Law Journal* 73 (2): 288–308.

Wentz, E. A. 2000. A shape definition for geographic applications based on edge, elongation, and perforation. *Geographical Analysis* 32 (2): 95–112.

Williams, E. A., and E. A. Wentz. 2008. Pattern analysis based on type, orientation, size, and shape. *Geographical Analysis* 40 (2): 97–122.

Xie, F., and D. Levinson. 2007. Measuring the structure of road networks. *Geographical Analysis* 39 (3): 336–56.

Young, H. P. 1988. Measuring the compactness of legislative districts. *Legislative Studies Quarterly* 13 (1): 105–15.

Zhao, Z. Q., and R. R. Stough. 2005. Measuring similarity among various shapes based on geometric matching. *Geographical Analysis* 37 (4): 410–22.

Zhu, X., and P. Byrt. 2013. Spatial analysis of ophthalmology patient catchments in Victoria, Australia. *Proceedings of the Surveying & Spatial Sciences Conference*. http://sssi.org.au/userfiles/docs/SSSI%20 General/documents_1368661687143997 6353.pdf

Correspondence: GeoDa Center for Geospatial Analysis and Computation, School of Geographical Sciences and Urban Planning, Arizona State University, Tempe, AZ 85287-5302, e-mail: wenwen@asu.edu (Li); wentz@asu.edu (Wentz); cfan13@asu.edu (Fan); Department of Physics, Arizona State University, Tempe, AZ 85287-1504, e-mail: tingyong.chen@asu.edu (Chen).